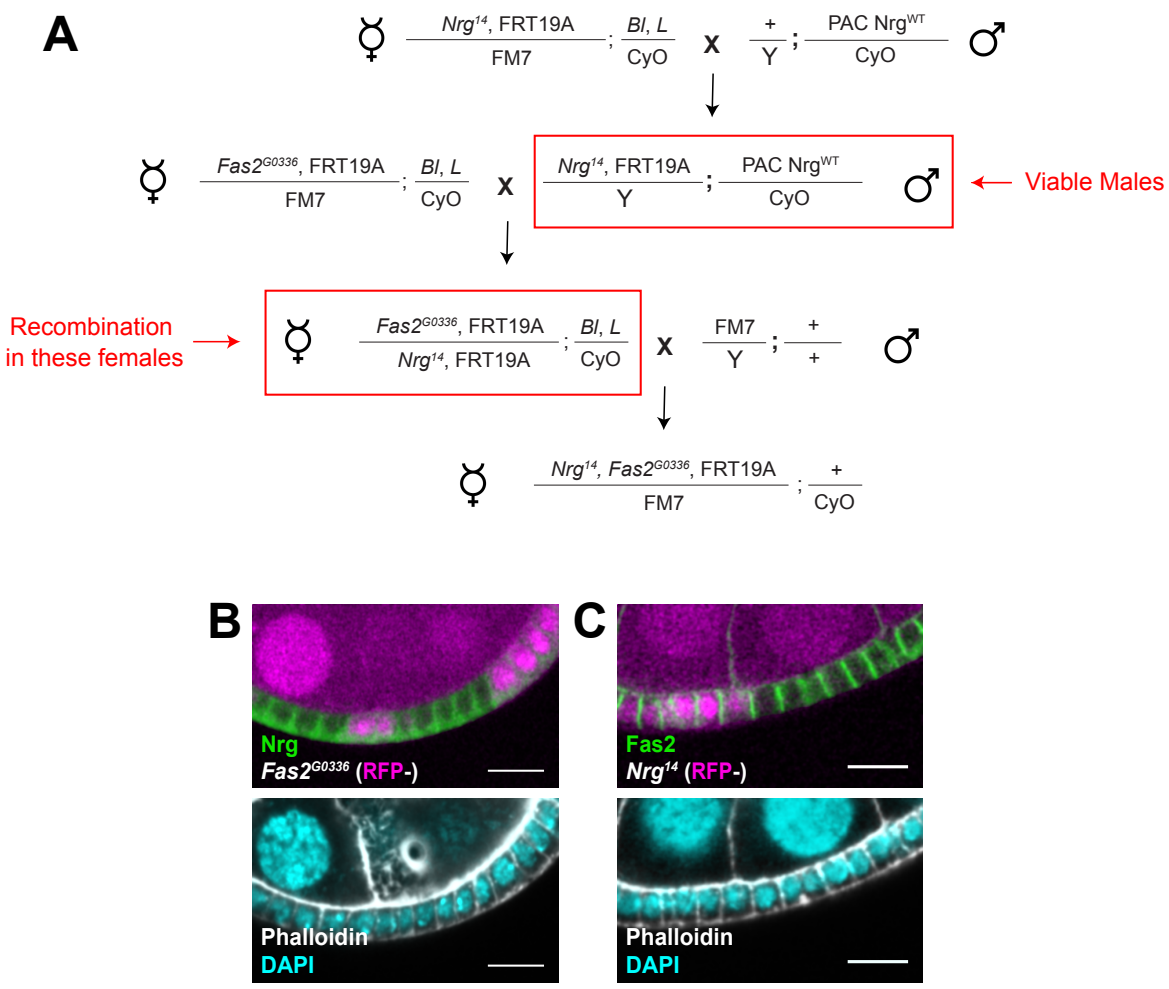

Figure S1. Nrg and Fas2 localization are not dependent on each other. Related to Figure 1. **A)** Crossing scheme for the generation of a *Nrg^{14}, Fas2^{G0336}* double mutant chromosome. Expression of full length Nrg from a genomic rescue construct (P1-derived artificial chromosome Nrg^{WT}) on the second chromosome allowed for fertile, viable male flies carrying the lethal null allele *Nrg^{14}*. **B)** Nrg localization, as measured by immunostaining, is unchanged in *Fas2^{G0336}* mutant follicle cell clones. **C)** Fas2 localization is unchanged in *Nrg^{14}* mutant follicle cell clones.

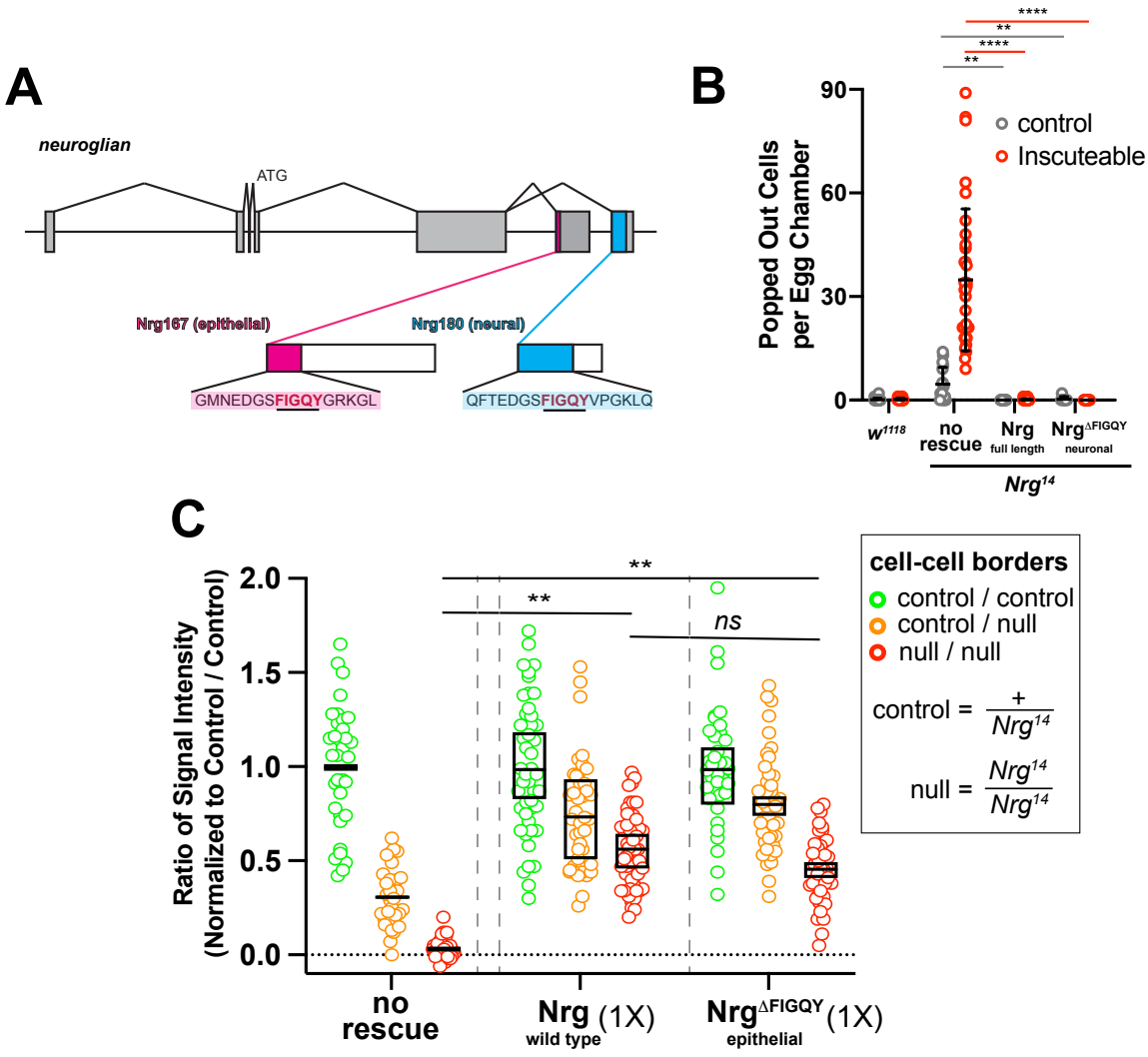

Figure S2. Deletion of the neuronal FIGQY domain of Nrg does not disrupt reintegration. Related to Figure 2.

A) Overview of the genomic locus of *nrg*. The Nrg167 (epithelial)- and Nrg180 (neural)-specific exons and the relevant amino acid sequences are depicted. The isoform-specific FIGQY sequences are highlighted in red. Adapted from Fig 2A Enneking et al (2013). B) Expression of Nrg with a deletion in the FIGQY subsequence of the Neuronal isoform produces an unchanged copy of Nrg in the follicular epithelium. Rescuing a *nrg* null mutant with this construct provides a full rescue as would be expected. Significance was determined using an unpaired, two-tailed student's t-test with Welch's correction. p-values left to right: $p = 0.0014$, $p < 0.0001$, $p = 0.0014$, $p < 0.0001$. C) Quantification of Nrg (signal intensity relative to local background) in null and rescue clones. Nrg was visualized by immunostaining. In all conditions, signal intensity

correlates with gene dosage; intensity is reduced by ~100% at a null/null border (red, left), but only ~50% when either one copy of Nrg^{WT} or $Nrg^{\Delta FIGQY}$ (epithelial) is expressed in all cells (orange, middle and right). Importantly, total gene dosage in the unrescued condition (1:1, 1:0, 0:0) is not the same in the rescue conditions (2:2, 2:1, 1:1). Signal intensity was normalized against the mean intensity of the control/control condition (green). Therefore, comparisons between genotypes reflect ratios rather than absolute pixel intensity. Statistical tests between egg chambers were performed using an unpaired two-tailed student's t-test. Circles represent individual cell-cell borders. Boxes represent minimum, maximum, and average intensities at the egg chamber level. p-values from left to right: $p = 0.0013$, $p = 0.0054$, $p = 0.16$.

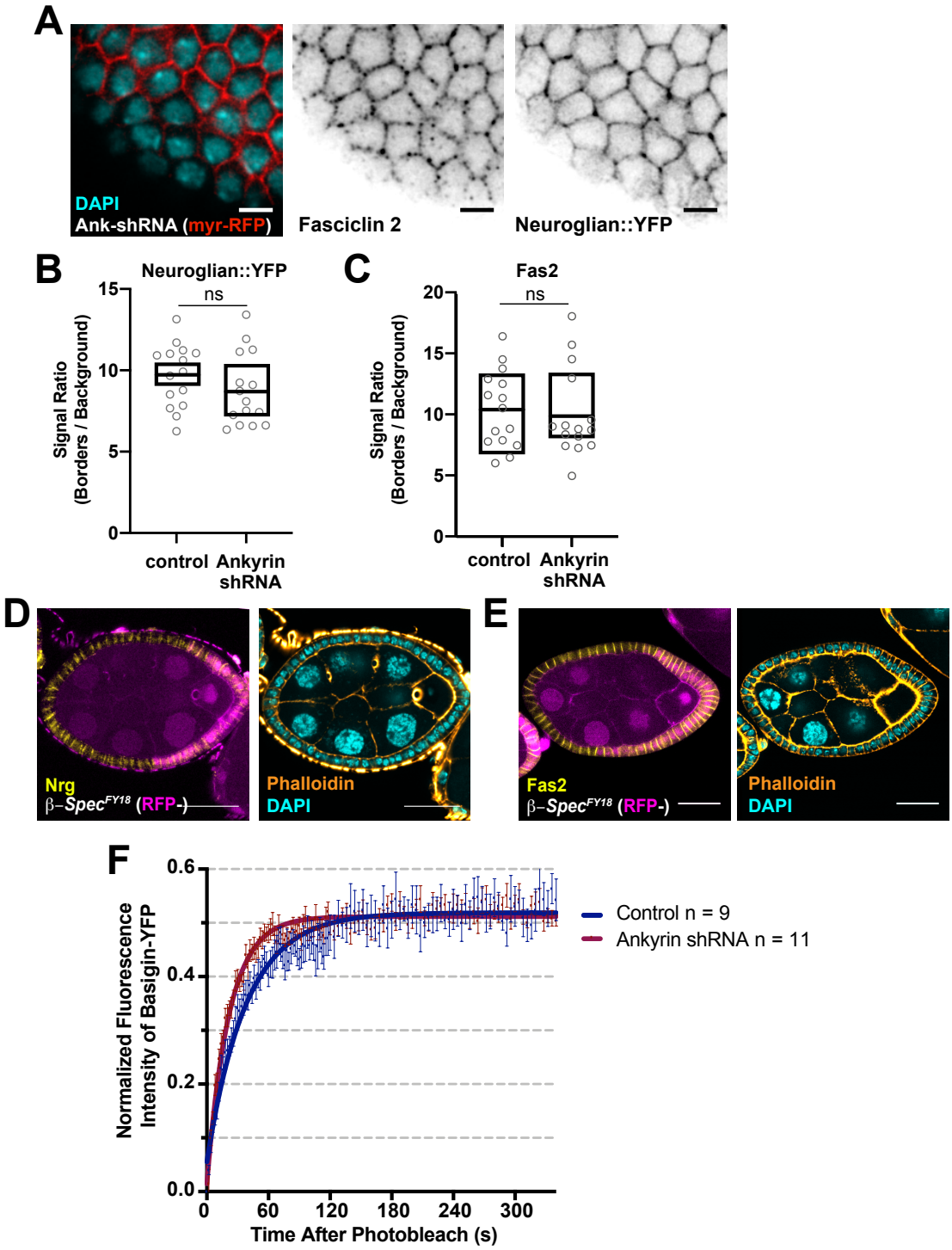

Figure S3. Fas2 and Nrg localizations are not affected by the loss of Ankyrin or β-spectrin. Related to Figure 3.

A) Fas2 and Nrg::YFP localization and expression are unchanged by knockdown of Ankyrin. Mosaic expression of UAS-Ankyrin-shRNA and UAS-myrisotylated-RFP (as a marker) were

driven in the FE by GR1-GAL4. Fas2 was visualized with the 1D4 antibody. **B and C)** Quantification of Nrg::YFP (A) and Fas 2 (B) signal (relative to local background) at cell borders in egg chambers expressing Ankyrin-shRNA driven by Traffic Jam-GAL4 or egg chambers with the driver alone (control). Three cell-cell borders were measured per egg chamber. Circles represent individual cell-cell borders. Boxes represent minimum, maximum, and average intensities at the egg chamber level. Significance was determined using an unpaired, two-tailed student's t-test with Welch's correction. p = 0.2098 in B; p = 0.0.7291 in C. **D and E)** Nrg and Fas2 localization and expression, as measured by immunostaining, is unchanged in β-*Spec*^{FY18} mutant follicle cell clones. **F)** Fluorescence recovery curves of Bsg::YFP after photobleaching. Lateral FE cell junctions were bleached in egg chambers expressing Ankyrin-shRNA driven by Traffic Jam-GAL4 or egg chambers with the driver alone (control). Fluorescence intensity was normalized to account for inherent photobleaching due to imaging. Experiments were performed independently with number of experimental repeats indicated. Curves were calculated by fitting a one phase association curve. Error bars represent SEM. The 95% confidence interval (CI) of the control plateau is 51-53. This overlaps with the 95% CI of the Ankyrin-shRNA plateau, which is 51-52.

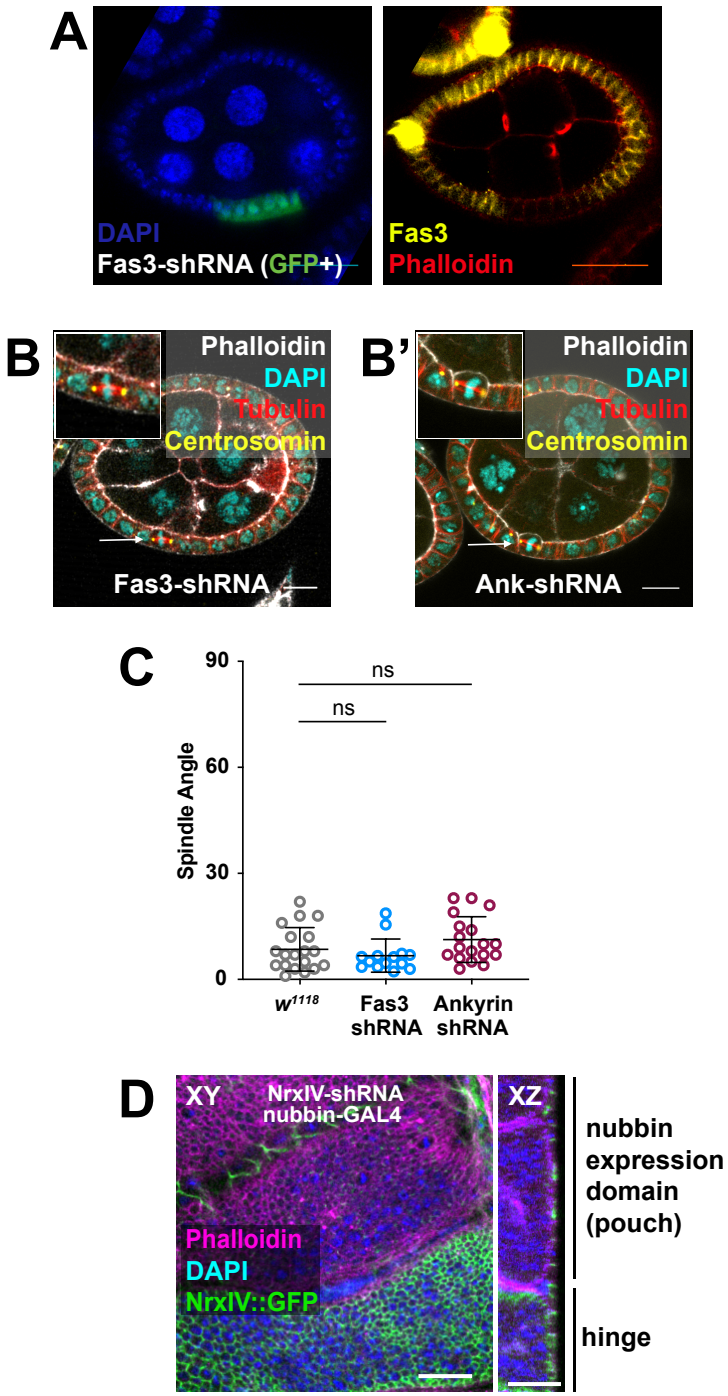

Figure S4. Verification of Fas3 and NrxIV knockdown and test for spindle orientation effects. Related to Figure 4.

A) Knockdown of Fas3 expression by shRNA reduces anti-Fas3 immunoreactivity. Fas3 localizes to cell-cell borders during the proliferative stages of follicle cell development. Fas3 is not observed

in cells expressing Fas3-shRNA (GFP+). In this experiment, both UAS-GFP and UAS-Fas3-shRNA are driven by Actin-GAL4, which is activated by mitotic recombination-based removal of a stop codon (Flp-out). **B)** Neither disruption of Ankyrin (B) nor Fas3 (B') affects mitotic spindle angle in the follicular epithelium. **C)** Quantification of spindle angles. Mitotic spindles have a mean angle of ~10° relative to the apical surface. Average and error bars represent mean and SD. Significance was determined using an unpaired, two-tailed student's t-test with Welch's correction. p-values left to right: $p = 0.3489$, $p = 0.1944$. **D)** Knockdown of NrxIV expression by shRNA reduces protein expression as measured by fluorescent signal intensity. NrxIV-shRNA was expressed under control of nubbin-Gal4 (expression domain indicated) in the imaginal wing discs of NrxIV::GFP larvae.

Figure 1D- Number of Egg Chambers		
	Control	+Inscuteable
Control	25	22
Nrg^{14}	17	34
$Fas2^{G0336}$	17	19
Nrg^{14}, $Fas2^{G0336}$	22	11
Figure 2A- Number of Egg Chambers		
Control	25	
$Fas2^{G0336}$	17	
$Fas2^{G0336}$ + Nrg^{WT}	12	
$Fas2^{G0336}$ + $Fas2^{TJGal4}$	14	
$Fas2^{G0336}$ + $Fas2Intra^{TJGal4}$	13	
$Fas2^{G0336}$ + $Fas2Extra^{TJGal4}$	16	
Nrg^{14}	17	
Nrg^{14} + $Fas2^{TJGal4}$	11	
Nrg^{14} + Nrg^{WT}	11	
Nrg^{14} + $Nrg^{167\Delta FIGQY}$	10	
Nrg^{14}, $Fas2^{G0336}$	22	
Nrg^{14}, $Fas2^{G0336}$ + $Fas2^{TJGal4}$	27	
Nrg^{14}, $Fas2^{G0336}$ + Nrg^{WT}	14	
Nrg^{14}, $Fas2^{G0336}$ + $Nrg^{167\Delta FIGQY}$	28	
Figure 2C- Number of Egg Chambers		
Control	22	
$Fas2^{G0336}$	19	
$Fas2^{G0336}$ + Nrg^{WT}	13	
Nrg^{14}	34	
Nrg^{14} + Nrg^{WT}	25	
Nrg^{14} + $Nrg^{167\Delta FIGQY}$	24	
Figure 3B- Number of Egg Chambers		
	Control	Ank shRNA
Control	25	21
Nrg^{14}	17	21
$Fas2^{G0336}$	17	13

Figure 3D- Number of Borders			
Control (5 ECs)		8	
Ankyrin shRNA (7 ECs)		9	
Figure 4B-Number of Egg Chambers			
		Control	Fas3 shRNA
Control		25	30
Nrg^{14}		17	28
Fas2^{G0336}		17	39
Figure 4E- Number of Borders			
Follicular Epithelium		20	
Wing Disc		20	
Figure 4F- Number of Egg Chambers			
		Control	NrxIV shRNA
Control		25	15
Nrg^{14}		17	20
Fas2^{G0336}		17	12
Figure S2B- Number of Egg Chambers			
		Control	Inscuteable
Control		25	22
Nrg^{14}		17	34
Nrg^{14} + Nrg^{WT}		11	25
Nrg^{14} + Nrg$^{180\Delta FIGQY}$		7	10
Figure S2C- Number of Borders			
	WT/WT	WT/Mutant	Mutant/Mutant
Nrg^{14} (2 ECs)	35	33	40
Nrg^{14}+Nrg^{WT} (3 ECs)	47	43	56
Nrg^{14}+Nrg$^{167\Delta FIGQY}$ (3 ECs)	37	43	43
Figure S3B- Number of Borders			
Control (5 ECs)		14	
Ankyrin shRNA (5 ECs)		15	
Figure S3C- Number of Borders			
Control (5 ECs)		15	
Ankyrin shRNA (5 ECs)		15	

Figure S3F- Number of Borders	
Control (6 ECs)	9
Ankyrin shRNA (8 ECs)	11
Figure S4C- Number of Spindles	
Control	19
Fas3 shRNA	14
Ank shRNA	18

Table S1. Sample numbers for each experiment. Related to STAR Methods.